# Antibody-mediated delivery of TAPBPR enables the redirection of virus-specific T cell responses to tumour cells

**Andreas Neerincx** (andreas.neerincx@googlemail.com)
University of Cologne
**Aure Aflalo** (aure.aflalo@gmail.com)
University of Cambridge https://orcid.org/0000-0002-7158-6868
**Ida Hafstrand** (ih339@cam.ac.uk)
University of Cambridge https://orcid.org/0000-0002-1012-9532
**Alice Abreu Torres** (at678@cam.ac.uk)
University of Cambridge
**Alison McDowall** (am2612@cam.ac.uk)
University of Cambridge https://orcid.org/0000-0003-2018-1462
**Arwen Altenburg** (afa34@cam.ac.uk)
University of Cambridge
**Reem Satti** (rs999@cam.ac.uk)
University of Cambridge
**F Ilca** (tudor.ilca@outlook.com)
University of Cambridge
**Klaus Okkenhaug** (ko256@cam.ac.uk)
University of Cambridge https://orcid.org/0000-0002-9432-4051
**Mark Wills** (mrw1004@cam.ac.uk)
University of Cambridge
**Louise Boyle** (lhb22@cam.ac.uk)
University of Cambridge https://orcid.org/0000-0002-3105-6555

**Article**

**Keywords:**

**DOI:** https://doi.org/

**Additional Declarations: Yes** there is potential Competing Interest. A patent has been filed based on this work: Patent applicant - Cambridge Enterprise; Name of inventors - Andreas Neerincx, F. Tudor Ilca and Louise H Boyle; Patent Application number - WO2019/145509; Status of application - filed.

# Antibody-mediated delivery of TAPBPR enables the redirection of virus-specific T cell responses to tumour cells

**Andreas Neerincx[1+], Aure Aflalo[1+], Ida Hafstrand[1], Alice Abreu Torres[1], Alison McDowall[1], Arwen F Altenburg[1], Reem Satti[1], F. Tudor Ilca[1], Klaus Okkenhaug[1], Mark Wills[2], and Louise H Boyle[1*]**

1 Department of Pathology, Tennis Court Road, University of Cambridge, Cambridge, UK CB2 1QP

2 Department of Medicine, University of Cambridge, Cambridge, UK

+ Contributed equally to the work

* corresponding author

**Abstract**

Low tumour immunogenicity is a major hurdle to overcome in the treatment of cancers with immunotherapies. Here, we reveal a novel therapeutic approach to increase tumour immunogenicity. By delivering the major histocompatibility complex class I (MHC-I) peptide exchange catalyst TAPBPR in an antibody-mediated manner onto the plasma membrane of tumour cells, extracellular MHC-I become highly peptide-receptive. Upon exposure to low doses of exogenous peptide, MHC-I molecules on tumour cells are efficiently loaded with immunogenic antigens, including those derived from human cytomegalovirus and Epstein-Barr virus. TAPBPR-antibody fusion proteins were delivered specifically to tumours *in vivo*. Finally, antigen-specific CD8+ T cells respond to tumour cells in a targeted manner and can mediate killing of antibody target-positive cells. As memory T cells specific for previously encountered common viruses patrol tumours, TAPBPR-based therapeutics could offer an attractive means to redirected virus-specific T cells against tumours in the fight against cancer.

## Introduction

While immunotherapies such as immune checkpoint inhibition have revolutionised the treatment of cancer, clinical benefit is currently only observed in a minority of patients.

High tumour mutational load is positively correlated with response to immunotherapy [1-6]. This exemplifies the role that immunogenic peptide presentation on MHC class I (MHC-I) molecules to CD8+ cytotoxic T cells plays in inducing effective antitumour immune responses. To broaden the clinical application of immunotherapy, innovative approaches are needed to overcome low immunogenicity of tumours frequently observed in patients.

Previously, we demonstrated that the MHC-I peptide editor TAPBPR can be exploited to decorate cells with immunogenic peptides [7]. While TAPBPR is typically expressed intracellularly and shapes the MHC-I immunopeptidome [8-10], we established that human recombinant soluble TAPBPR (sTAPBPR), comprising only the lumenal region, was able to perform peptide exchange directly on plasma membrane-expressed MHC-I (**Figure 1A**) [7]. Exogenous peptide loading onto MHC-I by sTAPBPR occurred in a peptide affinity-dependent manner [7]. Having used this system to further explore molecular aspects of TAPBPR function [11,12], we turned our attention as to whether sTAPBPR can be utilised to overcome the low immunogenicity of tumours. Here, we fuse the lumenal region of TAPBPR to antibody fragments with specificity to target proteins expressed on the plasma membrane of tumours (**Figure 1B**). We show that sTAPBPR can be specifically delivered to tumour cells expressing a target of interest and utilised to promote immunogenic peptide presentation onto human leukocyte antigen (HLA) molecules, including peptides derived

55 from human cytomegalovirus (HCMV) and Epstein-Barr virus (EBV), inducing virus-specific

56 cytotoxic T cell responses in a targeted manner.

## Results

### Tethering TAPBPR to a plasma membrane target protein

As human sTAPBPR can load neo-epitopes and virus-derived peptides directly on extracellular MHC-I [7] (**Figure 1A**), we explored ways to tether sTAPBPR to the plasma membrane of a target cell population. We explored whether functional sTAPBPR could be delivered to a target protein via its conjugation to a C-terminal antibody tag (**Figure 1B**). GFP was chosen as model target protein and was cloned into an expression vector designed to direct it onto the plasma membrane (**Figure 2A, Supplementary Text 1** for sequence), which, when transduced into cells, proved successful (**Figure 2B**).

As a tool compound, a sTAPBPR-nanobody fusion protein was made by cloning a nanobody specific for GFP ($GFP_{NB}$) downstream of sTAPBPR and a linker sequence (GGGGS x3) with a C-terminal 6xhis-tag included to permit protein purification (**Figure 2C, Supplementary Figure 1A, Supplementary Text 1** for sequence). Extremely high levels of TAPBPR-$GFP_{NB}$ binding were observed to HeLaM cells expressing the nanobody target (**green solid line, Figure 2D & 2E**) compared to the low levels of binding of sTAPBPR observed using the conditions tested (**blue lines, Figure 2D & 2E**). Negligible binding of the TAPBPR-$GFP_{NB}$ was observed to cells lacking surface GFP (**green dashed line, Figure 2D & 2E**). Shortening the linker between sTAPBPR and the nanobody to GGGGS or altering it to GSTVAAPSTVAAPSTVAAPSGS [13,14] did not significantly change the binding of TAPBPR-$GFP_{NB}$ to cells (**Supplementary Figure 1A & B, Supplementary Text 1**). A significant difference in TAPBPR binding to cells expressing the nanobody target compared to cells lacking the target was even observed when the concentration of TAPBPR-$GFP_{NB}$ was lowered from 100 nM to 10 or 1 nM (**Figure 2E**). Targeted delivery of the TAPBPR-$GFP_{NB}$ fusion protein was observed on the following cell

lines engineered to express GFP on their plasma membrane, but not their GFP-negative counterparts: HeLaM-HLA-ABC$^{KO}$ cells overexpressing HLA-A*02:01 (HeLa A2 cells) (**Supplementary Figure 2A & 2B**); the mouse tumour cell line EL4 (**Supplementary Figure 3A-3C**); and the human breast cancer cell line MCF-7 (**Supplementary Figure 4A & 4B**). Together, these findings suggest that TAPBPR binding to cells can be directed specifically to a molecular target using a C-terminal antibody tag.

**Nanobody fusion permits MHC-I-independent tethering of TAPBPR**

We tested whether TAPBPR-GFP$_{NB}$ binding was mainly driven by nanobody:target engagement and to what extent the MHC-I binding site on TAPBPR contributed to the overall interaction. While no TAPBPR-GFP$_{NB}$ binding was observed to cells lacking HLA-A, -B and -C expression in the absence of surface GFP, TAPBPR-GFP$_{NB}$ binding to MHC-I-knockout cells was significantly enhanced upon surface GFP expression (**Figure 2F**). Thus, the nanobody:target interaction alone can mediate plasma membrane-tethering of TAPBPR. When surface GFP was introduced into wild-type (WT) HeLaM cells expressing endogenous MHC-I, TAPBPR-GFP$_{NB}$ binding was even higher (**Figure 2F**). Notably, HeLaM cells express HLA-A*68:02, the MHC-I allotype with the strongest binding to human TAPBPR tested to date [11]. Thus, recombinant sTAPBPR can be tethered to the plasma membrane via the nanobody:target interaction and this may be further enhanced when MHC-I is expressed. In the absence of the nanobody target, MHC-I expression played no role in TAPBPR-GFP$_{NB}$ binding to cells (**Figure 2F**). On MHC-I expressing cells lacking surface GFP, the binding of TAPBPR-GFP$_{NB}$ to cells was actually lower than that observed for sTAPBPR (**Figure 2F**). This

suggests that the MHC-I binding site on TAPBPR is only accessible upon fusion protein tethering to the cell surface via the nanobody.

**Plasma membrane tethered TAPBPR is highly efficient at mediating MHC-I peptide exchange**

We tested if TAPBPR-$GFP_{NB}$ promoted MHC-I peptide exchange when tethered to the plasma membrane by treating target cells with TAPBPR-$GFP_{NB}$ or sTAPBPR, followed by washing to remove unbound protein, then incubating with selected fluorescent peptides with high affinity for an MHC-I allotype expressed on the cells. This revealed that tethered TAPBPR retained its ability to perform peptide exchange and that it was a superior peptide exchange catalyst compared to sTAPBPR on three MHC-I allotypes tested; HLA-A*68:02 (**Figure 3A-D** & **Supplementary Figure 5**), HLA-A*02:01 (**Figure 3E, Supplementary Figure 2C, 2D** & **4C**), and murine H2-$K^b$ (**Supplementary Figure 3D & 3E**).

For example, using a fluorescent variant of the cancer neoantigen ETVSEQSNV (ETVSK*QSNV – were *denote a TAMRA labelled lysine residue) [15], extremely high levels of peptide binding were observed on HLA-A*68:02 when TAPBPR-$GFP_{NB}$ was plasma membrane-tethered to GFP (**green solid line Figure 3A, 3B and 3D, green bars Figure 3C**). Peptide binding was negligible on TAPBPR-$GFP_{NB}$ treated cells lacking the nanobody target (**green dashed line, Figure 3A, 3B and 3D, green bars Figure 3C)**, similar to treatment with peptide alone (**grey lines or bars Figure 3A, 3C, and 3D**). Only low ETVSK*QSNV binding to HLA-A*68:02 was observed using sTAPBPR (**blue lines Figure 3A, 3B and 3D, blue bars**

**Figure 3C)**. Unsurprisingly, here sTAPBPR exhibited less peptide exchange (following removal of excess unbound TAPBPR) compared to previously studies where sTAPBPR was left in excess [7,11]. This fits with the proposed allosteric-release mechanism for TAPBPR which suggests TAPBPR-mediated peptide exchange is impeded unless in high excess during the reaction [16]. Thus, tethering appears to concentrate TAPBPR at a high enough levels to mediate effective peptide exchange even following washing. The lack of peptide binding on cells lacking classical MHC-I expression (**Figure 3C**), suggests loading occurs directly on MHC-I (rather than via endocytosis), in agreement with previous findings [7]. Thus, plasma membrane tethered TAPBPR causes extracellular HLA-A*68:02 (**Figure 3D**) and -A*02:01 (**Figure 3E**) molecules to become $10^4$-$10^6$-fold more receptive to exogenous peptide loading.

**Functional TAPBPR can be delivered to tumours *in vivo***

Given the potential of TAPBPR-fusion technology to turn immunologically "cold" tumours "hot", we tested whether TAPBPR could be delivered to target-positive tumours *in vivo*. In mice bearing subcutaneous syngeneic EL4 lymphomas expressing surface GFP, TAPBPR-$GFP_{NB}$ was readily detected in tumours 15 min post-infusion with ~35% remaining 360 min post-infusion (predicted half-life of TAPBPR-$GFP_{NB}$ in tumour = 130 min) (**Figure 4A & 4B**). TAPBPR-$GFP_{NB}$ was not detected in the lungs of treated animals while extremely low levels were detected in the spleen (**Figure 4A**). At initial time-points, TAPBPR-$GFP_{NB}$ was readily detected in the kidney and liver (**Figure 4A**). However, TAPBPR-$GFP_{NB}$ levels in these two organs reduced rapidly with approximately 8% and 4%, respectively, remaining at 360 min post-infusion (predicted half-lives: kidney = 58 min, liver = 22 min)(**Figure 4A & 4B**). TAPBPR-$GFP_{NB}$ detection in liver and kidney is likely due to liver metabolism and renal

clearance of unbound protein. Indeed, evidence of cleaved TAPBPR is clearly observed using western blot analysis in the kidney samples (**Figure 4A**).

*Ex vivo* peptide exchange assays revealed tumoral TAPBPR-$GFP_{NB}$ promoted peptide loading onto nanobody target-positive tumour cells (**Green bars, Figure 4C**), but not on nanobody target-negative cells found in the tumours i.e. infiltrating immune cells and stroma (**Black bars, Figure 4C**). This suggests that TAPBPR is tethered to the tumour cells in a nanobody target-mediated manner and maintains its MHC-I peptide exchange catalyst functionality *in vivo*. There was no evidence of TAPBPR-$GFP_{NB}$-mediated peptide exchange in any of the organs tested (**Supplementary Figure 6A**), suggesting that TAPBPR-$GFP_{NB}$ detected in the liver and kidney was not functional.

**T cell recognition of peptides loaded by tethered TAPBPR**

While sTAPBPR is released upon facilitating MHC-I peptide loading, resulting in peptide:MHC-I complexes being available for T cell recognition [7], tethered TAPBPR remains plasma membrane-bound following MHC-I release. Thus, we explored whether peptides loaded onto MHC-I by tethered TAPBPR were available for T cell detection. SIINFEKL-specific, H2-$K^b$-restricted OT-1 T cell activation (CD69 expression), IFN-γ-expression and degranulation (CD107a expression) were all significantly enhanced in response to GFP+ target cells treated with TAPBPR-$GFP_{NB}$ prior to incubation with SIINFEKL peptide, compared to GFP- target cells treated with TAPBPR-$GFP_{NB}$ and peptide or peptide-pulsed EL4 cells in the absence of TAPBPR-$GFP_{NB}$ pretreatment (**Figure 4 D-F, Supplementary Figure 6 B-D)**.

Thus, peptides loaded onto MHC-I by tethered TAPBPR are available for CD8+ T cell recognition, and capable of triggering T cell activation, cytokine production and release of lytic granules to target-positive tumour cells.

**Induction of virus-specific T cells responses and killing target cells in a directed manner**

Virus-specific CD8+ T cells, including HCMV and EBV-specific T cells, are known to patrol tumours [17-22], opening up the potential of using these cells in cancer immunotherapy. Thus, we explored whether tethered TAPBPR induced human virus-specific T cells to respond to human cells in a targeted manner. Using HCMV-specific T cells that recognize the pp65-derived peptide NLVPMVATV in the context of HLA-A2 [23], a significant enhancement in IFN-y secretion from T cells was observed when surface GFP+ tumour cells were pretreated with TAPBPR-$GFP_{NB}$ before incubation with NLVPMVATV peptide (**green bars, Figure 5A**) compared to surface GFP+ tumour cells treated with the peptide alone (**grey bars, Figure 5A**) (~22-fold increase in the presence of tethered TAPBPR) or when peptide was loaded by sTAPBPR (**blue bars, Figure 5A**). Furthermore, it was comparable to the responses observed when the pp65 antigen was processed naturally by the target cells (**yellow bar, Figure 5A**). Moreover, a significant increase in T cell activation was observed when primary CD8+ T cells, isolated from blood of a HCMV+ HLA-A2+ individual, were incubated with tumour cells treated with tethered TAPBPR and NLVPMVATV peptide compared to tumour cells treated with peptide alone (**Figure 5B**).

For a more physiologically relevant system, we explored tethered TAPBPR's ability to induce virus-specific T cells to respond to autologous fibroblasts with matched MHC expressed at natural levels. Surface GFP was introduced into the fibroblasts to permit TAPBPR-$GFP_{NB}$ tethering and NLVPMVATV peptide binding in a target-dependent manner (**Supplementary Figure 7A-D**). Autologous NLVPMVATV-specific, HLA-A2 restricted CD8+ T cells showed a significant increase in IFN-γ production and release of lytic granules (as measured by CD107a surface expression) to GFP+ fibroblasts treated with TAPBPR-$GFP_{NB}$ and low dose peptide (10 or 100 nM), compared to GFP+ fibroblasts treated with low dose peptide alone, or GFP- fibroblasts treated with TAPBPR-$GFP_{NB}$ fusion protein and low dose peptide (**Figure 5C-E**, **Supplementary Figure 7E**).

Using co-culture assays with a mixture of GFP+ and GFP- fibroblasts, the ability of TAPBPR-$GFP_{NB}$ to facilitate virus-specific T cell-mediated killing of the fibroblasts was tested. In the absence of peptide or presence of 10 nM NLVPMVATV alone the ratio of live GFP+:GFP- fibroblasts remained unchanged following incubation with T cells (**Figure 5F, black and grey bars**). In contrast, when the mixed fibroblasts were treated with TAPBPR-$GFP_{NB}$ and 10 nM peptide in the presence of T cells there was significant depletion of the GFP+ fibroblasts compared to the GFP- fibroblasts (**Figure 5F, green bar**), which was comparable to the positive control in which the GFP+, but not the GFP- fibroblasts, were pulsed with 10 μM NLVPMVATV prior to T cell incubation (**Figure 5F, yellow bar**). Therefore, from a T cell perspective, tethered TAPBPR can make target cells resemble a virus-infected cell in the presence of low concentrations of exogenous virus-derived peptide, inducing virus-specific CD8+ T cells to respond and kill cells in a targeted manner.

## Tethering functional TAPBPR to HER2

Having achieved proof-of-concept using GFP as a model target protein and TAPBPR-$GFP_{NB}$ protein as a tool compound (**Figures 2-5**), we next determined whether similar results could be achieved by targeting TAPBPR to a *bona fide* tumour-specific marker. Human epidermal growth factor receptor 2 (HER2), a marker commonly overexpressed on breast cancer cells and the therapeutic antibody trastuzumab target [24], was selected as a tumour marker. A TAPBPR-anti-HER2 fusion protein was produced by cloning a HER2-specific single chain variable fragment downstream of soluble TAPBPR (TAPBPR-HER2-scFv) (**Figure 6A, Supplementary Text 1** for sequence). To test whether TAPBPR binding to tumour cells could be achieved in a HER2-specific manner, we either knocked-out or overexpressed HER2 in HeLaM cells (**Supplementary Figure 8A**). When HeLaM cells were incubated with TAPBPR-HER2-scFv, TAPBPR binding occurred in a HER2-dependent manner (**Figure 6B, Supplementary Figure 8B & 8C**). HER2-tethered TAPBPR retained its peptide exchange functionality and loaded peptide onto MHC-I in a HER2-dependent manner (**Figure 6C, Supplementary Figure 8D-8H**). Similar results were observed with fusion proteins containing alternative linker sequences between the sTAPBPR and HER2-scFv domain (**Supplementary Figure 9A-D, Supplementary Table 1**).

## HER2-tethered TAPBPR makes tumours look like virus-infected cells

Finally, we tested TAPBPR-HER2-scFv's ability to load immunogenic peptide on the breast cancer cell line SKBR3, which has high HER2 but low HLA-A2 expression (**Supplementary Figure 9E**). TAPBPR-HER2-scFv bound to SKBR3 cells (**Figure 6D, Supplementary Figure 9F**) and promoted the loading of fluorescent derivatives of the EBV-derived peptide YLLEMLWRL

and the HCMV-derived peptide NLVPMVATV onto the breast cancer line (**Figure 6E, Supplementary Figure 9G**). Staining with a T cell receptor (TCR)-like mAb specific for YLLEMLWRL:HLA-A2 complexes confirmed the significant increase in viral peptide:MHC-I complexes on the plasma membrane of SKBR3 cells upon treatment with TAPBPR-HER2-scFv (**Figure 6F, Supplementary Figure 9H**). The virus-derived peptides loaded onto SKBR3 by TAPBPR-HER2-scFv were recognized directly by virus-specific CD8+ T cells (**Figure 6G**). Together, these data demonstrate that TAPBPR can be tethered to HER2 to make tumour cells look like virus-infected cells triggering a CD8+ T cell response.

## Discussion

Low immunogenicity of tumours is a key issue to overcome to widen the application of cancer immunotherapy. While this is often due to low mutational burden of tumours [25], it also arises when tumours develop mechanisms to limit antigen presentation [26,27]. A further hurdle for immunotherapy is the variability in peptide presentation from patient to patient and tumour to tumour [28,29]. While current attempts to turn immunologically "cold" tumours "hot" include combining immunotherapy with radiotherapy [30], using oncolytic viruses to induce adjuvanticity [31] and epigenetic modulation to increase immunogenicity [32], new approaches to increase tumour immunogenicity are desperately needed.

Here, we reveal a novel way to override MHC-I peptide presentation in a targeted manner. Physiologically, TAPBPR functions intracellularly as an MHC-I peptide exchange catalyst [9,10] and chaperone [33], widening the MHC-I peptide binding groove at the α2-1 helix [34,35] to promote sub-optimal peptide release. TAPBPR release from MHC-I is triggered upon high affinity peptide binding onto MHC-I [7,16]. Here, by creating TAPBPR-antibody fragment fusion proteins, we can tether TAPBPR to plasma membrane-expressed target proteins. We show that tethered TAPBPR retains its ability to function as an MHC-I peptide editor. Compared to soluble TAPBPR, tethered TAPBPR is significantly more efficient at loading immunogenic peptides onto plasma membrane MHC-I molecules due to its ability to remain bound to the cell surface, thus enabling sequential binding to multiple MHC-I molecules. Peptides loaded onto MHC-I by TAPBPR-antibody fusions are accessible to antigen-specific CD8+ T lymphocytes. Serendipitously, TAPBPR-antibody fusion protein

design resulted in masking of the MHC-I binding site on TAPBPR in the non-bound state. Consequently, the TAPBPR-antibody fusions do not bind to cells lacking the target, suggesting limited off-target effects on healthy cells that express MHC-I but lack the antibody target. Furthermore, our work suggests the ability to deliver functional TAPBPR-antibody fusions specifically to target-positive tumours *in vivo*.

While loading antigenic peptide onto plasma membrane-expressed MHC-I can be achieved experimentally via peptide pulsing, it's a very inefficient process typically requiring high concentrations of peptide for a prolonged period limiting its broad clinical application. Our innovation enhances dissociation of endogenous peptide from plasma membrane-expressed MHC-I and stabilises MHC-I in a peptide-receptive conformation. Subsequent addition of exogenous MHC-I binding peptides results in target cell decoration extremely quickly and even with picomolar concentrations of peptides. While here we have demonstrated functional TAPBPR directed to GFP and HER2 expressing tumours, the platform nature of our technology opens the possibility to target different tumour types via specificity of the antibody domain.

This technology could have significant potential in cancer treatment to directly decorate tumours with a broad range of immunogenic tumour-specific and/or tumour-associated antigens to trigger tumour antigen-specific T cell responses. Excitingly, it also gives rise to the opportunity to make tumours look like virus-infected cells to turn virus-specific T cells against tumours in the fight against cancer. T cells induced by previously encountered common virus infections including influenza virus, HCMV and EBV patrol tumours [17-22].

While some of these virus-specific T cells may exhibit cross-reactivity to tumour antigens [20], they are generally considered to be bystander cells. Their abundance in tumours highlights that many tumour-infiltrating lymphocytes are not tumour specific. Intratumoral injection of high concentrations of peptide has demonstrated that antiviral memory T cells can be repurposed to limit tumour growth [17]. Furthermore, using antibody-conjugates to deliver peptide to tumours redirected HCMV-specific T cell responses towards tumours [36]. Through its catalytic peptide exchange action directly on plasma membrane MHC-I molecules, TAPBPR-based technologies offer an attractive means to bring peptide-based therapeutic approaches closer to the clinic.

## Methods

### Cell lines

The following human and mouse cell lines were used: HEK-293T cells, HeLaM cells [37] (both gifts from Paul Lehner, University of Cambridge, UK), the human breast cancer cell line MCF-7 (a kind gift from Sanjeev Kumar, CRUK Cambridge Institute), the HER2 overexpressing mammary breast adenocarcinoma cell line SKBR3 (a kind gift from Masashi Narita, CRUK Cambridge Institute) and the mouse lymphoma cell line EL4 (TB-39, ATCC). In addition, HeLaM in which HLA-A, -B and -C had been knocked-out [38], their HLA-A2 transduced counterparts [38] and HLA-A2+ HeLaM cells transduced with pp65 [7] were also used. Cell lines were maintained in DMEM (Sigma-Aldrich) supplemented with 10% FBS (Gibco, Thermo Fisher Scientific), 100 U/mL penicillin, and 100 μg/mL streptomycin (Gibco, Thermo Fisher Scientific) at 37 °C with 5% $CO_2$.

Dermal fibroblasts, obtained from a healthy, HCMV positive, HLA-A2 positive donor using the method described in [39], were TERT-transformed [40] then maintained in DMEM (Sigma-Aldrich) supplemented with 20% FBS (Gibco, Thermo Fisher Scientific), 100 U/mL penicillin, and 100 μg/mL streptomycin (Gibco, Thermo Fisher Scientific) at 37 °C with 5% $CO_2$.

### Constructs containing target protein sequences

eGFP was amplified from the lentiviral vector pHRSIN-C56W-UbEM [8] then cloned into pDisplay™ Mammalian Expression Vector (Invitrogen™) which targets and anchors proteins of interest to the cell surface using a N-terminal secretion signal (IgK leader sequence) and

the C-terminal transmembrane anchoring domain of platelet-derived growth factor receptor (PDGFR) (See **Supplementary Text 1** for the sequence of the eGFP-pDisplay protein). Subsequently, the coding region of eGFP-pDisplay was cloned into the lentiviral vector pHRSINcPPT-SGW. Human HER2 WT was amplified from Addgene plasmid # 16257 (http://n2t.net/addgene:16257 ; RRID:Addgene_16257) a gift from Mien-Chie Hung [41], and cloned into the lentiviral vector pHRSIN-C56W-UbEM (see **Supplementary Text 1** for sequence of HER2 WT).

To produce cells expressing GFP or HER2 on their plasma membrane, the lentiviral vector eGFP-pDisplay-pHRSINcPPT-SGW or HER2-pHRSIN-C56W-UbEM were transfected into HEK-293T cells along with the packaging vector pCMVΔR8.91 and the envelope vector pMD.G using Fugene (Promega). Supernatants containing lentiviral particles were collected at 48 h and were used to transduce target cells.

**Constructs to generate TAPBPR-antibody fusion proteins**

Vectors to produce sTAPBPR in the piggyBac system have previously been described [7]. To create the TAPBPR-$GFP_{NB}$ fusion proteins, a GFP nanobody sequence was amplified from pGEX6P1-GFP-Nanobody, a gift from Kazuhisa Nakayama (Addgene plasmid # 61838 ; http://n2t.net/addgene:61838 ; RRID:Addgene_61838)[42]. The forward primer used to amplify the GFP nanobody incorporated a PmlI restriction site, the nucleotide sequence encoding the short linker sequence, GGGGS, and a SpeI restriction site upstream of the GFP nanobody sequence, while the reverse primer used added a 6xHis tag downstream of the

nanobody. The resultant linker-$GFP_{NB}$-6xHis nucleotide product was subsequent annealed to the nucleotides encoding the lumenal region of TAPBPR then cloned into a piggyBac transposon-based mammalian cell expression system [43]. To create TAPBPR fusion products with altered linkers, restriction digest was used to remove the GGGGS linker from the TAPBPR-$GFP_{NB}$ vector, then primers encoding amino acid sequence GGGGSx3 [14] or GSTVAAPSTVAAPSTVAAPSGS [13] were annealed into the cut vector (see **Supplementary Text 1** for sequence of the three TAPBPR-$GFP_{NB}$ fusion proteins produced).

To create the TAPBPR-HER2-scFv fusion proteins, a HER2-specific scFv sequence was amplified from pACgp67B-Her2, a gift from Judy Lieberman (Addgene plasmid # 10794 ; http://n2t.net/addgene:10794 ; RRID:Addgene_10794)[44]. The sequence encoding the HER2-scFv was subsequently cloned into the TAPBPR-$GFP_{NB}$-piggyBac vectors in place of the $GFP_{NB}$ sequence (see **Supplementary Text 1** for sequence of the three TAPBPR-HER2-scFv fusion proteins produced).

**Expression and purification of TAPBPR proteins**

To produce secreted form of either sTAPBPR, the TAPBPR-$GFP_{NB}$ or TAPBPR-HER2-scFv fusion proteins, 293T cells were cotransfected in six-well plates with 0.9 μg of the TAPBPR containing PB-T-PAF vector along with 0.15 μg of both PB-RN and PBase (at a ratio of 6:1:1) [43]. 48 h after transfection, cells were grown in selection media (DMEM supplemented with 10% FBS, 1% pen/strep, 3 μg/mL puromycin (Invivogen), and 700 μg/mL geneticin (Thermo Fisher Scientific)) for 5 days. To induce TAPBPR protein expression, cells were

grown in DMEM supplemented with 5% FBS, 1% pen/strep, and 2 µg/mL doxycycline (Sigma-Aldrich). After 7 d, the media was collected and the TAPBPR protein was purified using Ni-NTA affinity chromatography (HisTrap$^{TM}$ excel, Cytiva) on a Äkta Start system (Cytiva). After elution the buffer was exchanged to PBS and the protein was concentrated using a Vivaspin 20 30000 MWCO PES concentrator (Sartorius) and purified using a HiLoad$^{R}$ 16/600 Superdex$^{TM}$ 75 pg size exclusion column (Cytiva).

**HER2 knockout in HeLaM cells**

Depletion of HER2 was achieved using the sgRNA sequence CACTTGGGTGCTCGCGGCTC cloned into pSpCas9 (BB)-2 A-puro [37]. To generate HER2 knockout cells, HeLaM were transfected with the HER2-CRISPR plasmid in the absence of serum using Lipofectamine2000 (Invitrogen, Thermo Fisher Scientific). 24 h after transfection, the medium was replaced with complete DMEM containing 2 µg/mL puromycin (Invivogen, San Diego, CA). After 48 h, the medium was replaced with complete DMEM without puromycin.

**Antibodies**

The following primary antibodies were used: ab290, a rabbit polyclonal specific for GFP (Abcam, UK); PeTe4, a mouse monoclonal antibody (mAb) specific for the native conformation of human TAPBPR [8] that does not cross-react with tapasin [45]); Anti-TAPBPR antibody [OTI1C9] raised against recombinant full length protein corresponding to Human TAPBPR (ab236419, Abcam); 25D-1.16, which recognises H-2K$^{b}$ complexed with $OVA_{257–264}$ (SIINFEKL) peptide (Thermofisher); The rabbit anti-calnexin polyclonal (ADI-SPA-

860, Enzo Life Sciences); the mouse IgG2a isotype control (X0943, Sigma-Aldrich); Alexa Fluor 488 anti-HER2 (CAT 324410, Biolegend); APC-anti-mouse CD107a (121614, Biolegend): APC-Cy7-anti-mouse CD69 (104526, Biolegend); PE-anti-mouse IFN-γ (505808, Biolegend); Alexa Fluor 647 anti-human CD107a (328611, Biolgend); TCR-like mAb L1, which recognises the EBV-derived peptide $LMP_{1125–133}$ (YLLEMLWRL) in association with HLA-A*02:01 [46](a kind gift from Paul MacAry, National University of Singapore, Singapore). The following secondary antibodies were used: Goat anti-mouse Alexa Fluor 647 IgG (A21236, Invitrogen Molecular Probes, Thermo Fisher Scientific); Goat anti-rabbit Alexa Fluor 647 (A21244, Invitrogen Molecular Probes, Thermo Fisher Scientific); IgG Goat anti-mouse IRDye 880 cw (926-32219, LiCor); Goat anti-rabbit IRDye 680 rd (926-68071, LiCor).

**MHC-I-binding peptides**

The following MHC-I-specific peptides were used: a fluorescent derivative of the HLA-A*68:02-binding peptide ETVSEQSNV (a neoepitope from the elongation factor 2 gene) [15], ETVSK*QSNV, where K* represents a lysine labelled with 5-carboxytetramethylrhodaime (TAMRA)]; The immunogenic HLA-A*02:01-binding peptide NLVPMVATV (derived from the human CMV protein pp65) [23], together with its fluorescently-labelled variant NLVPK*VATV; a fluorescent derivative of the CCR4-NOT transcription complex subunit 1 YVVPFVAKV, YVVPFVAK*V, which binds to HLA-A*02:01 and HLA-A*68:02 [7,9]; The immunogenic HLA-A*02:01-binding peptide YLLEMLWRL (derived from the EBV protein latent membrane protein 1)[46] together with its TAMRA labelled equivalent YLLEK*LWRL; The OVA-derived peptide SIINFEKL which binds to H-$2K^b$ and its TARMA-labelled variant SIINFEK*L. All peptides were purchased from Peptide Synthetics UK.

## *In vitro* TAPBPR binding & peptide binding assays

Cells were seeded on 12-well plate at 2.5-3.0 x $10^4$ cells/well and treated with 200 U/mL IFN-γ (Peprotech) for 48-72 h to upregulate MHC class I expression. Cells were washed with 1x PBS and then incubated in Opti-MEM (GIBCO, Thermo Fisher Scientific), at physiological pH, without or with the indicated concentration (1 pM- 100 nM) of sTAPBPR, TAPBPR-$GFP_{NB}$ or TAPBPR-HER2-scFv at 37°C for 15 min. Excess unbound TAPBPR was subsequently removed by washing 3 times in 1 x PBS. For TAPBPR binding assays, adherent cells were trypsinised, before bound TAPBPR was detected using the human TAPBPR-specific mAb, PeTe4, by flow cytometry. For peptide binding assays, fluorescently-labelled peptides were added to the cells at the indicated concentration (1 pM – 10 μM) for the indicated time (15 – 60 min). Cells were then washed three times in 1x PBS to remove any excess of unbound peptide. After cells were harvested, the level of fluorescent peptide bound was measured by flow cytometry.

## Measurement of target protein expression, TAPBPR binding and peptide loading using flow cytometry

Following trypsinization, cells were washed in 1% BSA, dissolved in 1× PBS at 4 °C. To detect fluorescent peptide bound to cells, samples were directly analysed by detecting TAMRA fluorescence. For the detection of surface target proteins (GFP, HER2), bound TAPBPR, YLLEMLWRL-loaded HLA-A*02:01 molecules or SIINFEKL-loaded H-$2K^b$, cells were stained for 30 min at 4 °C in PBS+1% BSA containing anti-GFP, anti-HER2, PeTe4, the TCR-like mAb L1 or 25-D1.16, respectively, or with an isotype control antibody. After washing the cells to remove excess unbound antibody, the primary antibodies bound to the cells were detected

by incubation at 4 °C for 30 min with Alexa-Fluor 647 goat anti-mouse or anti-rabbit IgG. After a subsequent round of washing, the fluorescence levels were detected using either a BD FACScan analyzer with Cytek modifications or using a BD Cytoflex S flow cytometer. Analysis was performed using FlowJo software (FlowJo).

**Animals**

C57BL/6 mice were bred and housed in accordance with United Kingdom Home Office regulations. All animal studies were ethically reviewed and carried out in accordance with the Animals (Scientific Procedures) Act 1986. Work was conducted under home office project licences by staff with a valid project licence.

***In vivo* delivery of TAPBPR-antibody fusion proteins**

8–9-week-old C57BL/6 mice were subcutaneous injected $5x10^5$ EL4 cells expressing surface GFP. At day 12, following tumour establishment, animals were infused i.v. with and 200 µg TAPBPR-$GFP_{NB}$ before tumours and organs were harvested 15-360 min post-infusion. As a control, mice were injected with PBS. Tumours were homogenised prepared using gentleMACS™ C Tubes (Miltenyi) and a gentleMACS™ Dissociator using the m-impTumour01_01 programme. Homogenised tumours and whole organs were mashed through a 70-µm cell strainer (Greiner) with a 2 ml syringe plunger to prepare single cell suspensions, which were then washed with PNS after centrifugation.

**Detection of TAPBPR-$GFP_{NB}$**

To detect TAPBPR-$GFP_{NB}$ in organ and tumours, cells were lysed in 1% Triton X-100 (VWR, Radnor, PN) in Tris-buffered saline (TBS) (20 mM Tris-HCl, 150 mM NaCl, 2.5 mM $CaCl_2$), supplemented with 10 mM NEM and protease inhibitor cocktail (cOmplete Mini, Roche, UK), for 30 min at 4°C. Nuclei and debris were removed by centrifugation at 20,000 x g for 15 min. Samples were heated at 99°C for 10 min in sample buffer (125 mM Tris-HCl pH 6.8, 4% SDS, 20% glycerol, 0.04% bromophenol blue) supplemented with 100 mM β-mercaptoethanol. Following separation by gel electrophoresis, proteins were transferred onto an nitrocellulose Amersham, Protran membrane (GE Healthcare). Membranes were blocked using 5% (w/v) dried milk and 0.1% (v/v) Tween 20 in PBS for 30 min, followed by incubation with the mouse anti-TAPBPR (OTI1C9) and rabbit anti-calnexin polyclonal (ADI-SPA-860) antibodies in blocking buffer at 4°C overnight. After washing, membranes were probed with LI-COR secondary antibodies at room temperature followed by imaging using the LI-COR Odyssey imaging system, according to the manufacturer's instructions. Protein bands from at least two independent immunoblots were quantified by using Odyssey software (LI-COR Biosciences).

### ***Ex vivo*** **peptide exchange assays**

To determine if functional TAPBPR had been delivered to tumours or the organs *in vivo*, *ex vivo* peptide exchange assays were performed. Single cell suspensions from tumours, liver, spleen, lung or kidney were incubated with 1 nM SIINFEK*L for 15 min at 37˚C. Following washing cells were stained with Zombie Aqua Fixable Viability kit (Biolegend) according to manufacturer's instructions. The samples were then fixed using 4% PFA and analysed on a BD Cytoflex S flow cytometer. During analysis, the GFP positive vs negative cells from

tumour samples were gated in order to differentiate EL4-GFP cells from stroma and immune cells, followed by analysis for TAMRA binding. The background autofluorescence of samples was subtracted from peptide treated samples.

**Isolation and stimulation of OT1 T cells**

Splenocytes were isolated from 8-12 week old C57BL/6 animals with OTI $Tcra^{Tg(TcraTcrb)110Mjb}$ and ubiquitous GFP Tg(UBC-GFP)30Scha/J transgenes and cultured in RPMI (Gibco) with 10% FBS (Gibco), 1% Penicillin/Streptomycin (Gibco), 2 mM L-glutamine (Gibco) and 50 µM beta-mercaptoethanol (Millipore) supplemented with 10nM SIINFEKL. After 48h, CD8+ T cells were sorted using the MoJoSort Mouse CD8 T cell isolation kit (Biolegend) according to the manufacturer's instructions and cultured for 6-8 days in culture medium supplemented with 40 ng/mL interleukin-2 (Peprotech).

**OT1 T cell activation assay**

EL4 cells -/+ surface GFP expression were harvested, washed and stained with 100nM CellTrace Violet (Invitrogen) for 20 min, washed, and incubated with 10 nM TAPBPR-$GFP_{NB}$ in Opti-MEM (Gibco) for 15min at 37°C. Cells were washed once with PBS and incubated with 100 pM SIINFEKL peptide in 200 µL Opti-MEM for 15min at 37°C. After a final wash the EL4 cells were resuspended in complete RPMI and co-cultured with OT1 T cells for 18 h at an effector:target ratio of 10:1. After 12h, the media was exchanged for fresh media containing 1:1500 GolgiStop (BD Biosciences) and 2µg/mL APC-anti-CD107a then incubated for another 6h. Subsequently, cells were stained with 1:1000 Zombie Yellow viability dye (423104, Biolegend) and 2µg/mL APC-Cy7-anti-CD69. Cells were then fixed and permeabilised using

the BD Cytofix/Cytoperm kit (554715, BD Biosciences) and stained with 2 µg/mL PE-anti-IFN-γ. Samples were acquired on a BD Cytoflex S flow cytometer and analysed using FlowJo.

**Human T cells**

Ethical approval was obtained from the Addenbrooke's National Health Service Hospital Trust Institutional Review Board (Cambridge Research Ethics Committee) for this study. Informed written consent was obtained from all donors in accordance with the Declaration of Helsinki (LREC 97/092). The expansion of HLA-A2 restricted NLVPMVATV (HCMV $pp65_{495–504}$) specific CD8+ T cells was performed as previously described [7].

**FluoroSpot T Cell Assays**

Target cells were stimulated with 200 U/mL IFN-γ for 48 h. Cells were then washed with PBS and incubated 100 nM sTAPBPR, TAPBPR-$GFP_{NB}$, TAPBPR-HER2-scFv or without TAPBPR in Opti-MEM for 15 min at 37°C. Cells were washed in PBS to remove excess unbound TAPBPR, then incubated with the indicated concentrations of NLVPMVATV peptide in Opti-MEM for 60 min at 37°C. F ollowing peptide treatment, target cells were washed in PBS and harvested, then resuspended in X-VIVO 15 (Lonza) or TexMACS (Miltenyi Biotech) media supplemented with 5% human serum at $1 \times 10^6$ cells/mL. Target cells were then irradiated for 20 min to cease proliferation throughout the experiment. 50,000 target cells were co-cultured with 8,000 NLVPMVATV specific CD8+ T cells or 37,500 primary CD8+ T cells in triplicate wells in coated Fluorospot plates [human IFN-γ FLUOROSPOT (Mabtech AB)], at 37 °C in a humidified $CO_2$ atmosphere for 20-24 h. The cells and medium were decanted from the plate and the assay developed following the manufacturer's instructions. Developed

plates were read using an AID iSpot reader (Autoimmun Diagnostika) and counted using EliSpot v7 software (Autoimmun Diagnostika).

**T cell degranulation assay**

Donor-matched TERT-transformed dermal fibroblasts and NLVPMVATV-specific CD8+ T cells were used to reduce background T cell activation. Target cells were stimulated with 200 U/mL IFNγ for 48-72 h to upregulate MHC-I expression. Target cells were harvested and washed in PBS, then incubated +/- 100 nM TAPBPR-$GFP_{NB}$ in Opti-MEM for 15 min at 37°C. After washing to remove excess unbound TAPBPR, targets were incubated with 0 nM, 10 nM, or 10 μM NLVPMVATV for 60 min at 37°C as indicated. Target cells were then washed in PBS and resuspended in RPMI supplemented with 10% human serum. T cells were incubated with $2x10^5$ target cells at an effector:target ratio of 1:1 in RPMI supplemented with 10% human serum in the presence of Alexa Fluor 647 anti-CD107a antibody and incubated at 37°C. After 1 h, Brefeldin A and monensin (1:1000, BD Biosciences) and the co-culture was allowed to proceed for a further 5 h. Cells were washed in PBS and stained with LIVE/DEAD™ Fixable Aqua Dead Cell Stain Kit (Invitrogen) for 20 min at 4°C. Samples were washed and fixed using Fluorofix Buffer (Biolegend) and acquired on an Attune NxT (ThermoFisher) flow cytometer.

**T cell killing assay**

Donor-matched TERT-transformed dermal fibroblasts and NLVPMVATV-specific CD8+ T cells were used to reduce background T cell activation. Target cells were stimulated with 200

U/mL IFNγ for 48-72 h to upregulate MHC-I expression. Target cells were harvested, , washed in PBS, and GFP- and GFP+ were mixed. Mixed target cells incubated +/- 100 nM TAPBPR-$GFP_{NB}$ in Opti-MEM for 15 min at 37°C. After washing to remove excess unbound TAPBPR, targets were incubated +/- 10 nM, NLVPMVATV for 60 min at 37°C as indicated. As a positive control, GFP+ cells alone were incubated with 10 μM NLVPMVATV before being mixed with untreated GFP- cells. Target cells were then washed in PBS, resuspended in RPMI supplemented with 10% human serum, and incubated with or without T cells at an effector:target ratio of 2.5:1 for 24 h at 37°C. Cells in suspension were removed from the culture plate, and the remaining attached fibroblasts were washed and incubated with LIVE/DEAD™ Fixable Far Red Dead Cell Stain Kit (Invitrogen) for 20 min at 4°C. Attached cells were then trypsinised and fixed, and acquired using an Accuri C6 flow cytometer (BD). Live cells were gated based on GFP expression to determine the ratio of surviving GFP- and GFP+ fibroblasts.

**Graphs and statistical analysis**

Graphs were generated using GraphPad Prism version 9.1.1, GraphPad Software, San Diego, California USA (www.graphpad.com). Statical analysis was performed using On Two-way ANOVA followed by multiple comparisons corrected using method of Benjamini, Krieger ad Yekutieli or a Tukey test. P values on graphs: n/s not significant, * P =0.01 to 0.05, **P ≤ 0.01, ***P ≤ 0.001, ****P ≤ 0.0001.

## Figure legends

### Figure 1 – Concept for TAPBPR-based therapeutics

**(A)** Cartoon depicting previous findings published in Ilca *et al*., 2018 [7]. Recombinant human TAPBPR (sTAPBPR), consisting of the lumenal domain only, added exogenously to cells binds to plasma membrane-expressed MHC-I and catalyses peptide dissociation, rendering MHC-I molecules into a peptide-receptive state. Upon incubation with exogenous "foreign" peptide, cells are subsequently decorated with peptide and are recognised by antigen-specific cytotoxic T cells. **(B)** Cartoon depicting proof-of-concept tested in this study. To explore whether TAPBPR can be utilised therapeutically, we attempted to deliver human TAPBPR in a targeted manner to the plasma membrane of tumours. To this end, TAPBPR was conjugated at its C-terminus with antibody fragments with specificity to target proteins expressed on tumours. We hypothesised that selective delivery of TAPBPR to target expressing cells could be achieved, which would lead to targeted decoration of cells, and consequently T cell recognition and killing of the targeted population e.g. tumour cells in an antigen-dependent manner.

### Figure 2 – TAPBPR can be tethered to a target protein on the plasma membrane

(**A**) Schematic of the construct to deliver GFP to the plasma membrane as a model antibody target protein. (**B**) Histogram showing surface expression of GFP on HeLaM cells -/+ transduction with eGFP-pDisplay. (**C**) Schematic of the TAPBPR-$GFP_{NB}$ fusion protein comprised of amino acids 1-391 of TAPBPR encoding the leader sequence and lumenal domain of human TAPBPR, followed by a linker region, a nanobody specific for GFP and a C-

589 terminal 6xHIS tag. The linker region used for the majority of experiments was
590 GGGGSGGGGSGGGGS. TAPBPR-$GFP_{NB}$ fusions with two other linkers were also created (see
591 **Supplementary Figure 1**). (**D**) Histogram and (**E**) line graph showing the binding of TAPBPR-
592 $GFP_{NB}$ and sTAPBPR to HeLaM with and without surface expression of GFP following
593 incubation with the indicated concentration of TAPBPR. (**F**) Bar chart showing TAPBPR
594 binding to HeLaM cells depleted of HLA-ABC molecules using CRISPR (MHC-I -) and WT
595 HeLaM cells expressing endogenous MHC-I (MHC-I +) both with and without surface GFP
596 (GFP+/-). Cells were incubated with 100 nM sTAPBPR or TAPBPR-$GFP_{NB}$. Error bars show -/+
597 SD of the mean fluorescence intensity (MFI) from three independent experiments.

598

599 **Figure 3 –TAPBPR tethered to the plasma membrane is highly efficient at mediating**
600 **peptide exchange on MHC-I molecules**

601 (**A**) Histogram and (**B-D**) graphs show the binding of ETVSK*QSNV (a fluorescent-derivative
602 of ETVSEQSNV) to HLA-A*68:02 molecules on surface GFP-negative or GFP-positive HeLaM
603 cells pretreated with either TAPBPR-$GFP_{NB}$, sTAPBPR or without any TAPBPR pretreatment,
604 as indicated. Panel C includes data on HeLaM HLA-$ABC^{KO}$ cells as a further control. Unless
605 indicated otherwise, 100 nM TAPBPR protein and 10 nM peptide was used. In **B**, TAPBPR
606 concentration was varied (1 pM–100 nM) while in **D** the concentration of ETVSK*QSNV
607 peptide was varied (1 pM-10 µM). (**E**) Line graph shows the binding of NLVPK*VATV (a
608 fluorescent derivative of the HCMV-derived peptide NLVPMVATV) to HLA-A2 molecules on
609 surface GFP-negative or GFP-positive HeLa A2 cells, pretreated with either TAPBPR-$GFP_{NB}$,
610 sTAPBPR or without any TAPBPR pretreatment as indicated over a range of peptide
611 concentrations (1 pM-10 µM). Error bars show -/+ SD of the mean fluorescence intensity

612 (MFI) from three independent experiments. Altering the linker sequence did not
613 significantly influence the ability of TAPBPR-GFP$_{NB}$ to promote exogenous peptide loading
614 onto MHC-I (**Supplementary Figure 1C**).

615

616 **Figure 4 - Functional TAPBPR can be delivered to tumours *in vivo* and T cells respond to**
617 **peptides loaded by tethered TAPBPR *in vitro***

618 C57BL/6 mice bearing EL4 tumours expressing surface GFP were infused with a single i.v.
619 infusion of 200 µg TAPBPR-GFP$_{NB}$ protein then culled at the indicated time-point (4 mice per
620 time-point), followed by harvesting of tumours and organs. (**A**) Western blot showing
621 representative images of TAPBPR-GFP$_{NB}$ detection in tumours and indicated organs using a
622 TAPBPR-specific monoclonal antibody (clone OTI1C9). Calnexin is included as a loading
623 control. (**B**) TAPBPR levels remaining in tumour, liver and kidney over time based
624 quantification of western blot images. The level of TAPBPR-GFP$_{NB}$ at 15 min in each
625 specimen was set to 100% and other time-points normalised accordingly. Error bars
626 represent -/+ SD from at least 2 independently repeated blotting experiments. (**C**) *Ex vivo*
627 peptide exchange on tumours following incubation of the single cell suspensions with 1 nM
628 SIINFEK*L for 15 min at 37˚C. Each point on the bar chart represents the fluorescent peptide
629 binding detected from an individual animal. In **C** the level of peptide loading on GFP+ and
630 GFP- tumour cells is shown. Error bars show -/+ SD of the MFI from three independent
631 experiments. (**D-F**) EL4 target cells -/+ surface GFP were incubated -/+ 10 nM TAPBPR-GFP$_{NB}$
632 for 15 min, followed by incubation -/+ 100 pM SIINFEKL peptide for 15 min before culturing
633 with OT1 T cells for 18 h at an E:T ratio of 10:1. (**D**) OT1 T cell activation (CD69 staining), (**E**)
634 IFN-γ expression and (**F**) degranulation (CD107a staining) were determined using flow

cytometry. Graphs show the percentage of OT1 T cells positive for the indicated marker. The MFI of CD69, IFN-γ and CD107a staining of OT1 T cells can be found in **Supplementary Figure 6**. The data is representative of two independent experiments performed in triplicate.

**Figure 5 – Tethered TAPBPR can load virus-derived peptides onto human tumour cells inducing T cell recognition and killing of tumours**

**(A & B)** HeLaM A2 cells expressing surface GFP or (**C-F**) fibroblast from an HCMV-positive, HLA-A2-positive donor -/+ surface GFP expression were treated with either no TAPBPR, 100 nM sTAPBPR or 100 nM TAPBPR-$GFP_{NB}$ as indicated for 15 min, and then incubated with the indicated concentration of NLVPMVATV peptide for 60 min. In **A-C**, following washing and irradiation, the target cells were cultured with either (**A**) donor-derived HLA-A2-restricted CD8+ T cells specific for the HCMV-derived peptide NLVPMVATV, (**B**) primary CD8+ T cells from an HCMV-positive, HLA-A2-positive individual or (**C**) autologous HLA-A2-restricted, NLVPMVATV-specific CD8+ T cells for 20-24h. Fluorospot assays measuring IFN-γ secretion were used to determine T cell activity. In **A**, a positive control of HeLaM A2 cells transduced with the HCMV protein pp65 was included to show the ability of the T cells to respond to the naturally-processed peptide while in **C** target cells were pulsed with 10 μM NLVPMVATV prior to co-culture acts as a positive control (yellow bars). Error bars show -/+ SD from triplicate wells and the data is representative of at least two independent experiments.

In **D-F**, following washing, the fibroblasts were co-cultured with autologous HLA-A2-restricted, NLVPMVATV-specific CD8+ T cells. (**D&E**) T cell degranulation (E:T=1:1) was measured by CD107a staining after 6h. As a positive control, target cells were pulsed with 10 μM NLVPMVATV prior to co-culture (yellow bars). The percentage of T cells which

degranulated was normalised to the positive control. **D** shows representative contour plots, and **E** shows means +/- SD of two independent experiments performed in duplicate. **(F)** After 24 h co-culture (E:T=2.5:1), target cells were harvested, the ratio of live GFP+/GFP- cells was determined and normalised to the ratio observed for each condition in the absence of T cells. As a positive control, GFP+, but not GFP- cells, were pulsed with 10 μM NLVPMVATV prior to mixing and co-culture (yellow bars). Error bars show -/+ SD from duplicate wells and the data is representative of three independent experiments.

**Figure 6 - TAPBPR can be tethered to HER2 to make tumour cells looks like virally infected cells**

**(A)** Schematic of TAPBPR-HER2-scFv fusion protein. Bar graphs showing (**B**) TAPBPR binding on a HeLaM cell panel with a range of HER2 expression levels treated with 100 nM TAPBPR-HER2-scFv for 15 min and (**C**) loading of peptide onto HLA-A*68:02 molecules when cells were subsequently incubated with 10 nM ETVSK*QSNV peptide. Representative histograms and binding of TAPBPR-HER2-scFv and ETVSK*QSNV at additional TAPBPR-HER2-scFv concentrations can be found in **Supplementary Figure 8**. (**D-G**) IFN-γ treated SKBR3 cells were incubated with or without 100 nM soluble TAPBPR or TAPBPR-HER2-scFv for 15 min at 37˚C, followed by: (**D**) detection of surface bound TAPBPR; (**E**) measuring MHC-I peptide loading following incubation with 10 nM fluorescent YLLEK*LWRL or NLVPK*VATV peptide for 60 min; (**F**) TCR-like mAb LMP-1 detection of YLLEMLWRL/HLA-A*02:01 complexes on the plasma membrane following incubation -/+ 10 nM nonlabelled YLLEMLWRL peptide for 60 min at 37˚C; (**G**) measuring IFN-γ from HLA-A2 restricted, NLVPMVATV-specific CD8+ T cells using Fluorospot assays following incubation -/+ 100 nM nonlabelled NLVPMVATV

peptide for 60 min. SKBR3 pulsed with 10 μM peptide is included as a positive control. Error bars show -/+ SD from triplicate wells. The data are representative of two independent experiments.

**Acknowledgements**

We thank Dr Grace Cooper (Department of Pathology, University of Cambridge) for helpful discussions regarding the OT1 T cell assay, Georgina Okecha (Department of Medicine, University of Cambridge) for provision of the HCMV-specific T cell line, Joana Cerveira (Department of Pathology, University of Cambridge) for helpful discussion regarding flow cytometry, Paul MacAry (National University of Singapore, Singapore) for the kind gift of the TCR-like mAb L1, and Crown Bioscience for performing the *in vivo* delivery of TAPBPR-$GFP_{NB}$ fusion protein. We acknowledge Henrietta Lack for HeLa cells. Finally, we thank the donors used to make the CMV specific T cell lines and fibroblasts. For the purpose of open access, the author has applied a CC BY public copyright licence to any Author Accepted Manuscript version arising from this submission.

**Funding**

A.N. was funded by a Wellcome Senior Research Fellowship [104647/Z/14/Z to L.H.B.]. A.A is funded by a Wellcome PhD studentship [220012/Z/19/Z], I.H was funded by a Cancer Research UK Immunology Project award [A25343], A.A.T, A.D, A.F.A are funded by Wellcome Senior Research Fellowship [219479/Z/19/Z to L.H.B], R.S is supported by a Department of Pathology PhD studentship, F.T.I was funded by a Wellcome PhD Studentship [109076/Z/15/A], M.R.W. is supported by Medical Research Council Grant [MR/K021087/1]. L.H.B was supported by Wellcome Senior Research Fellowships [104647/Z/14/Z and 219479/Z/19/Z]. This work was supported by a Medical Research Council Confidence in Concept grant [MRC MC_PC_17156].

## Author contributions

A.N – conception, experimental design, performed research, analysed data

A.A. – experimental design, performed research, analysed data, wrote the manuscript

I.H – experimental design, performed research, analysed data

A.A.T – performed research, analysed data

A.D, A.F.A, R.S, F.T.I – performed research

K.O – experimental design, resources, funding

M.R.W – supervision, resources, experimental design

L.H.B – conception, experimental design, analysed data, funding, supervision, wrote the manuscript.

## Rights retention statement



## Competing interests

A patent has been filed based on this work: Patent applicant - Cambridge Enterprise; Name of inventors - Andreas Neerincx, F. Tudor Ilca and Louise H Boyle; Patent Application number - WO2019/145509; Status of application - filed.

## References


1. Sharma P, Hu-Lieskovan S, Wargo JA, Ribas A: **Primary, Adaptive, and Acquired Resistance to Cancer Immunotherapy**. *Cell* 2017, **168**:707-723.
2. Rizvi NA, Hellmann MD, Snyder A, Kvistborg P, Makarov V, Havel JJ, Lee W, Yuan J, Wong P, Ho TS, et al.: **Cancer immunology. Mutational landscape determines sensitivity to PD-1 blockade in non-small cell lung cancer**. *Science* 2015, **348**:124-128.
3. Snyder A, Makarov V, Merghoub T, Yuan J, Zaretsky JM, Desrichard A, Walsh LA, Postow MA, Wong P, Ho TS, et al.: **Genetic basis for clinical response to CTLA-4 blockade in melanoma**. *N Engl J Med* 2014, **371**:2189-2199.
4. Van Allen EM, Miao D, Schilling B, Shukla SA, Blank C, Zimmer L, Sucker A, Hillen U, Geukes Foppen MH, Goldinger SM, et al.: **Genomic correlates of response to CTLA-4 blockade in metastatic melanoma**. *Science* 2015, **350**:207-211.
5. Lawrence MS, Stojanov P, Polak P, Kryukov GV, Cibulskis K, Sivachenko A, Carter SL, Stewart C, Mermel CH, Roberts SA, et al.: **Mutational heterogeneity in cancer and the search for new cancer-associated genes**. *Nature* 2013, **499**:214-218.
6. Hellmann MD, Callahan MK, Awad MM, Calvo E, Ascierto PA, Atmaca A, Rizvi NA, Hirsch FR, Selvaggi G, Szustakowski JD, et al.: **Tumor Mutational Burden and Efficacy of Nivolumab Monotherapy and in Combination with Ipilimumab in Small-Cell Lung Cancer**. *Cancer Cell* 2018, **33**:853-861 e854.
7. Ilca FT, Neerincx A, Wills MR, de la Roche M, Boyle LH: **Utilizing TAPBPR to promote exogenous peptide loading onto cell surface MHC I molecules**. *Proc Natl Acad Sci U S A* 2018, **115**:E9353-E9361.
8. Boyle LH, Hermann C, Boname JM, Porter KM, Patel PA, Burr ML, Duncan LM, Harbour ME, Rhodes DA, Skjodt K, et al.: **Tapasin-related protein TAPBPR is an additional component of the MHC class I presentation pathway**. *Proc Natl Acad Sci U S A* 2013, **110**:3465-3470.
9. Hermann C, van Hateren A, Trautwein N, Neerincx A, Duriez PJ, Stevanovic S, Trowsdale J, Deane JE, Elliott T, Boyle LH: **TAPBPR alters MHC class I peptide presentation by functioning as a peptide exchange catalyst**. *Elife* 2015, **4**:e09617.
10. Morozov GI, Zhao H, Mage MG, Boyd LF, Jiang J, Dolan MA, Venna R, Norcross MA, McMurtrey CP, Hildebrand W, et al.: **Interaction of TAPBPR, a tapasin homolog, with MHC-I molecules promotes peptide editing**. *Proc Natl Acad Sci U S A* 2016, **113**:E1006-1015.
11. Ilca FT, Drexhage LZ, Brewin G, Peacock S, Boyle LH: **Distinct Polymorphisms in HLA Class I Molecules Govern Their Susceptibility to Peptide Editing by TAPBPR**. *Cell Rep* 2019, **29**:1621-1632 e1623.
12. Ilca FT, Neerincx A, Hermann C, Marcu A, Stevanovic S, Deane JE, Boyle LH: **TAPBPR mediates peptide dissociation from MHC class I using a leucine lever**. *Elife* 2018, **7**:e40126.
13. Scott MJ, Lee JA, Wake MS, Batt KV, Wattam TA, Hiles ID, Batuwangala TD, Ashman CI, Steward M: **'In-Format' screening of a novel bispecific antibody format reveals significant potency improvements relative to unformatted molecules**. *MAbs* 2017, **9**:85-93.
14. Chen X, Zaro JL, Shen WC: **Fusion protein linkers: property, design and functionality**. *Adv Drug Deliv Rev* 2013, **65**:1357-1369.
15. Hogan KT, Eisinger DP, Cupp SB, 3rd, Lekstrom KJ, Deacon DD, Shabanowitz J, Hunt DF, Engelhard VH, Slingluff CL, Jr., Ross MM: **The peptide recognized by HLA-A68.2-restricted, squamous cell carcinoma of the lung-specific cytotoxic T lymphocytes is derived from a mutated elongation factor 2 gene**. *Cancer Res* 1998, **58**:5144-5150.
16. McShan AC, Natarajan K, Kumirov VK, Flores-Solis D, Jiang J, Badstubner M, Toor JS, Bagshaw CR, Kovrigin EL, Margulies DH, et al.: **Peptide exchange on MHC-I by TAPBPR is driven by a negative allostery release cycle**. *Nat Chem Biol* 2018, **14**:811-820.

17. Rosato PC, Wijeyesinghe S, Stolley JM, Nelson CE, Davis RL, Manlove LS, Pennell CA, Blazar BR, Chen CC, Geller MA, et al.: **Virus-specific memory T cells populate tumors and can be repurposed for tumor immunotherapy**. *Nat Commun* 2019, **10**:567.
18. Scheper W, Kelderman S, Fanchi LF, Linnemann C, Bendle G, de Rooij MAJ, Hirt C, Mezzadra R, Slagter M, Dijkstra K, et al.: **Low and variable tumor reactivity of the intratumoral TCR repertoire in human cancers**. *Nat Med* 2019, **25**:89-94.
19. Simoni Y, Becht E, Fehlings M, Loh CY, Koo SL, Teng KWW, Yeong JPS, Nahar R, Zhang T, Kared H, et al.: **Bystander CD8(+) T cells are abundant and phenotypically distinct in human tumour infiltrates**. *Nature* 2018, **557**:575-579.
20. Chiou SH, Tseng D, Reuben A, Mallajosyula V, Molina IS, Conley S, Wilhelmy J, McSween AM, Yang X, Nishimiya D, et al.: **Global analysis of shared T cell specificities in human non-small cell lung cancer enables HLA inference and antigen discovery**. *Immunity* 2021, **54**:586-602 e588.
21. Oliveira G, Stromhaug K, Klaeger S, Kula T, Frederick DT, Le PM, Forman J, Huang T, Li S, Zhang W, et al.: **Phenotype, specificity and avidity of antitumour CD8(+) T cells in melanoma**. *Nature* 2021, **596**:119-125.
22. Caushi JX, Zhang J, Ji Z, Vaghasia A, Zhang B, Hsiue EH, Mog BJ, Hou W, Justesen S, Blosser R, et al.: **Transcriptional programs of neoantigen-specific TIL in anti-PD-1-treated lung cancers**. *Nature* 2021, **596**:126-132.
23. Wills MR, Carmichael AJ, Mynard K, Jin X, Weekes MP, Plachter B, Sissons JG: **The human cytotoxic T-lymphocyte (CTL) response to cytomegalovirus is dominated by structural protein pp65: frequency, specificity, and T-cell receptor usage of pp65-specific CTL**. *J Virol* 1996, **70**:7569-7579.
24. Hudis CA: **Trastuzumab — Mechanism of Action and Use in Clinical Practice**. *New England Journal of Medicine* 2007, **357**:39-51.
25. Goodman AM, Kato S, Bazhenova L, Patel SP, Frampton GM, Miller V, Stephens PJ, Daniels GA, Kurzrock R: **Tumor Mutational Burden as an Independent Predictor of Response to Immunotherapy in Diverse Cancers**. *Mol Cancer Ther* 2017, **16**:2598-2608.
26. Jhunjhunwala S, Hammer C, Delamarre L: **Antigen presentation in cancer: insights into tumour immunogenicity and immune evasion**. *Nature Reviews Cancer* 2021, **21**:298-312.
27. Dersh D, Hollý J, Yewdell JW: **A few good peptides: MHC class I-based cancer immunosurveillance and immunoevasion**. *Nature Reviews Immunology* 2021, **21**:116-128.
28. Smith CC, Selitsky SR, Chai S, Armistead PM, Vincent BG, Serody JS: **Alternative tumour-specific antigens**. *Nature Reviews Cancer* 2019, **19**:465-478.
29. Yarchoan M, Johnson BA, 3rd, Lutz ER, Laheru DA, Jaffee EM: **Targeting neoantigens to augment antitumour immunity**. *Nat Rev Cancer* 2017, **17**:209-222.
30. Ngwa W, Irabor OC, Schoenfeld JD, Hesser J, Demaria S, Formenti SC: **Using immunotherapy to boost the abscopal effect**. *Nat Rev Cancer* 2018, **18**:313-322.
31. Zheng M, Huang J, Tong A, Yang H: **Oncolytic Viruses for Cancer Therapy: Barriers and Recent Advances**. *Mol Ther Oncolytics* 2019, **15**:234-247.
32. Dunn J, Rao S: **Epigenetics and immunotherapy: The current state of play**. *Mol Immunol* 2017, **87**:227-239.
33. Sagert L, Hennig F, Thomas C, Tampe R: **A loop structure allows TAPBPR to exert its dual function as MHC I chaperone and peptide editor**. *Elife* 2020, **9**:e55326.
34. Jiang J, Natarajan K, Boyd LF, Morozov GI, Mage MG, Margulies DH: **Crystal structure of a TAPBPR-MHC I complex reveals the mechanism of peptide editing in antigen presentation**. *Science* 2017, **358**:1064-1068.
35. Thomas C, Tampe R: **Structure of the TAPBPR-MHC I complex defines the mechanism of peptide loading and editing**. *Science* 2017, **358**:1060-1064.

36. Millar DG, Ramjiawan RR, Kawaguchi K, Gupta N, Chen J, Zhang S, Nojiri T, Ho WW, Aoki S, Jung K, et al.: **Antibody-mediated delivery of viral epitopes to tumors harnesses CMV-specific T cells for cancer therapy**. *Nat Biotechnol* 2020, **38**:420-425.
37. Tiwari RK, Kusari J, Sen GC: **Functional equivalents of interferon-mediated signals needed for induction of an mRNA can be generated by double-stranded RNA and growth factors**. *EMBO J* 1987, **6**:3373-3378.
38. Neerincx A, Boyle LH: **Preferential interaction of MHC class I with TAPBPR in the absence of glycosylation**. *Mol Immunol* 2019, **113**:58-66.
39. Poole E, Groves I, Jackson S, Wills M, Sinclair J: **Using Primary Human Cells to Analyze Human Cytomegalovirus Biology**. *Methods Mol Biol* 2021, **2244**:51-81.
40. Nakayama J, Tahara H, Tahara E, Saito M, Ito K, Nakamura H, Nakanishi T, Tahara E, Ide T, Ishikawa F: **Telomerase activation by hTRT in human normal fibroblasts and hepatocellular carcinomas**. *Nat Genet* 1998, **18**:65-68.
41. Li YM, Pan Y, Wei Y, Cheng X, Zhou BP, Tan M, Zhou X, Xia W, Hortobagyi GN, Yu D, et al.: **Upregulation of CXCR4 is essential for HER2-mediated tumor metastasis**. *Cancer Cell* 2004, **6**:459-469.
42. Katoh Y, Nozaki S, Hartanto D, Miyano R, Nakayama K: **Architectures of multisubunit complexes revealed by a visible immunoprecipitation assay using fluorescent fusion proteins**. *J Cell Sci* 2015, **128**:2351-2362.
43. Li Z, Michael IP, Zhou D, Nagy A, Rini JM: **Simple piggyBac transposon-based mammalian cell expression system for inducible protein production**. *Proc Natl Acad Sci U S A* 2013, **110**:5004-5009.
44. Song E, Zhu P, Lee SK, Chowdhury D, Kussman S, Dykxhoorn DM, Feng Y, Palliser D, Weiner DB, Shankar P, et al.: **Antibody mediated in vivo delivery of small interfering RNAs via cell-surface receptors**. *Nat Biotechnol* 2005, **23**:709-717.
45. Hermann C, Strittmatter LM, Deane JE, Boyle LH: **The binding of TAPBPR and Tapasin to MHC class I is mutually exclusive**. *J Immunol* 2013, **191**:5743-5750.
46. Sim AC, Too CT, Oo MZ, Lai J, Eio MY, Song Z, Srinivasan N, Tan DA, Pang SW, Gan SU, et al.: **Defining the expression hierarchy of latent T-cell epitopes in Epstein-Barr virus infection with TCR-like antibodies**. *Sci Rep* 2013, **3**:3232.

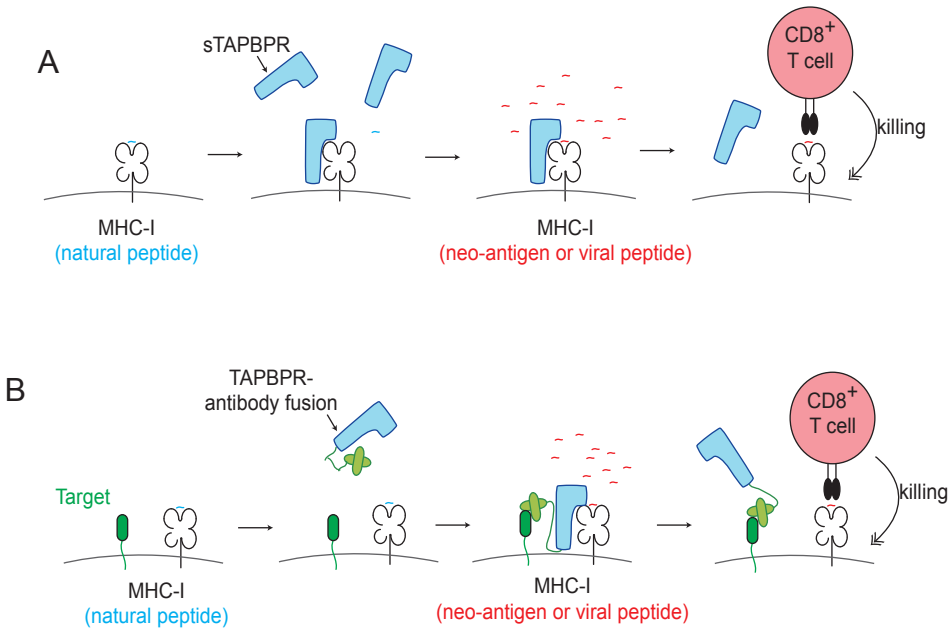
A
sTAPBPR
CD8+
T cell
killing
MHC-I
(natural peptide)
MHC-I
(neo-antigen or viral peptide)
B
TAPBPR-
antibody fusion
Target
CD8+
T cell
killing
MHC-I
(natural peptide)
MHC-I
(neo-antigen or viral peptide)

Figure 1

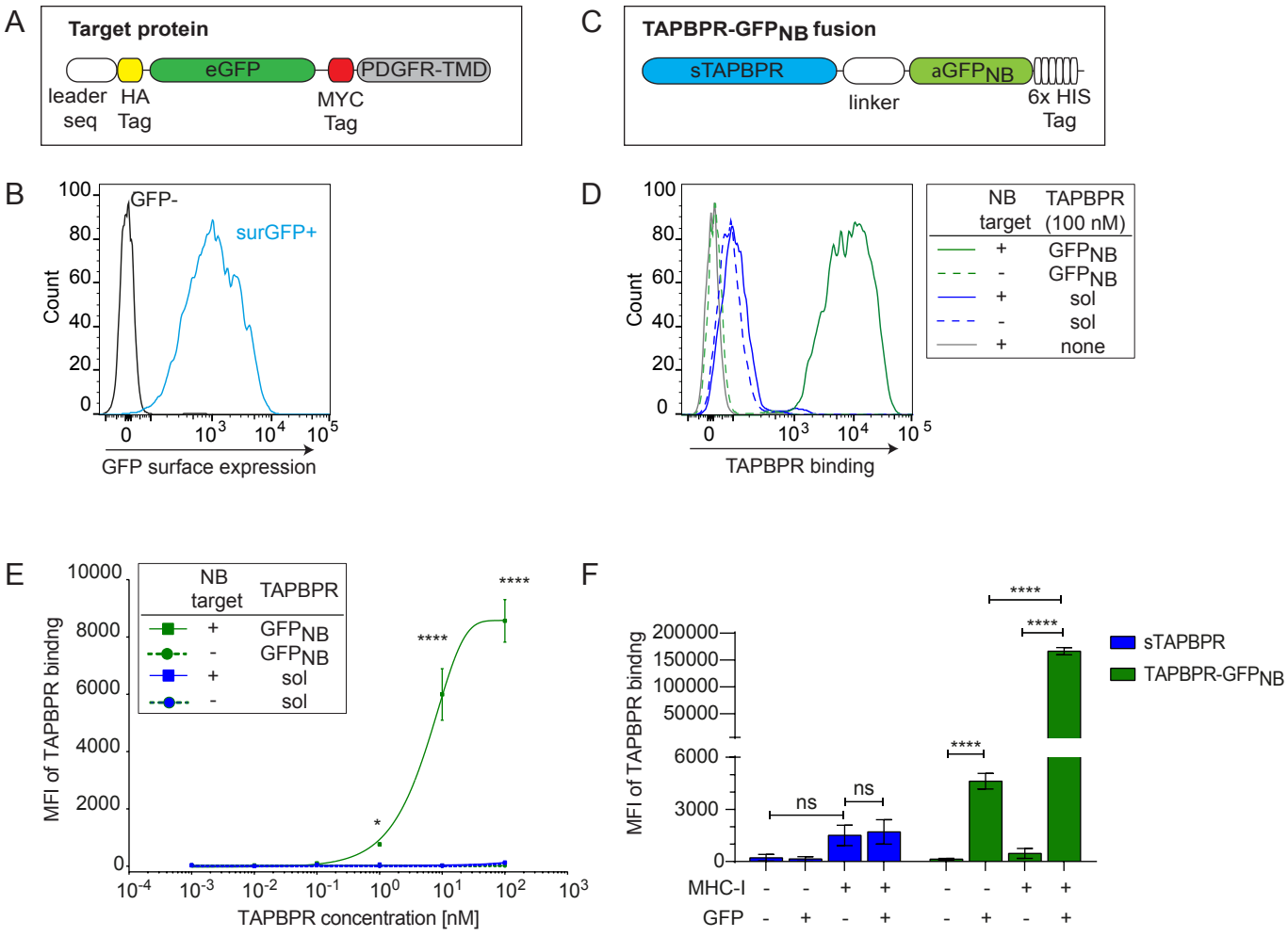
A
Target protein
leader seq
HA Tag
eGFP
MYC Tag
PDGFR-TMD
C
TAPBPR-GFPNB fusion
sTAPBPR
linker
aGFPNB
6x HIS Tag
B
GFP-
surGFP+
Count
GFP surface expression
D
Count
TAPBPR binding
NB target
TAPBPR (100 nM)
GFPNB
GFPNB
sol
sol
none
E
MFI of TAPBPR bindng
TAPBPR concentration [nM]
NB target
TAPBPR
GFPNB
GFPNB
sol
sol
F
MFI of TAPBPR bindng
MHC-I
GFP
ns
ns
sTAPBPR
TAPBPR-GFPNB

Figure 2

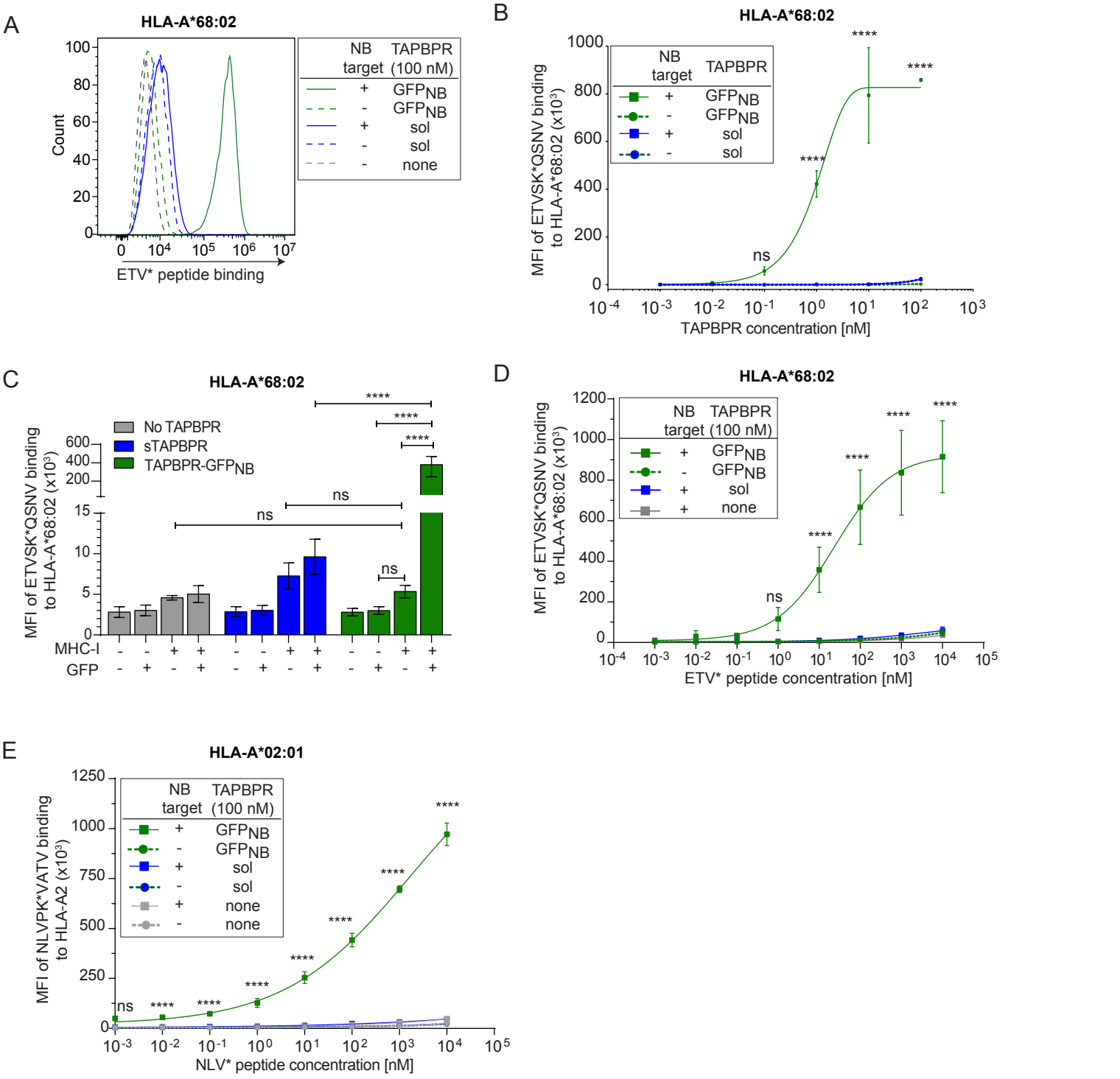
A
HLA-A*68:02
Count
ETV* peptide binding
NB target
TAPBPR (100 nM)
+ GFPNB
- GFPNB
+ sol
- sol
- none
B
HLA-A*68:02
MFI of ETVSK*QSNV binding to HLA-A*68:02 (x10³)
TAPBPR concentration [nM]
NB target
TAPBPR
+ GFPNB
- GFPNB
+ sol
- sol
ns
****
C
HLA-A*68:02
MFI of ETVSK*QSNV binding to HLA-A*68:02 (x10³)
No TAPBPR
sTAPBPR
TAPBPR-GFPNB
MHC-I
GFP
ns
****
D
HLA-A*68:02
MFI of ETVSK*QSNV binding to HLA-A*68:02 (x10³)
ETV* peptide concentration [nM]
NB target
TAPBPR (100 nM)
+ GFPNB
- GFPNB
+ sol
+ none
ns
****
E
HLA-A*02:01
MFI of NLVPK*VATV binding to HLA-A2 (x10³)
NLV* peptide concentration [nM]
NB target
TAPBPR (100 nM)
+ GFPNB
- GFPNB
+ sol
- sol
+ none
- none
ns
****

Figure 3

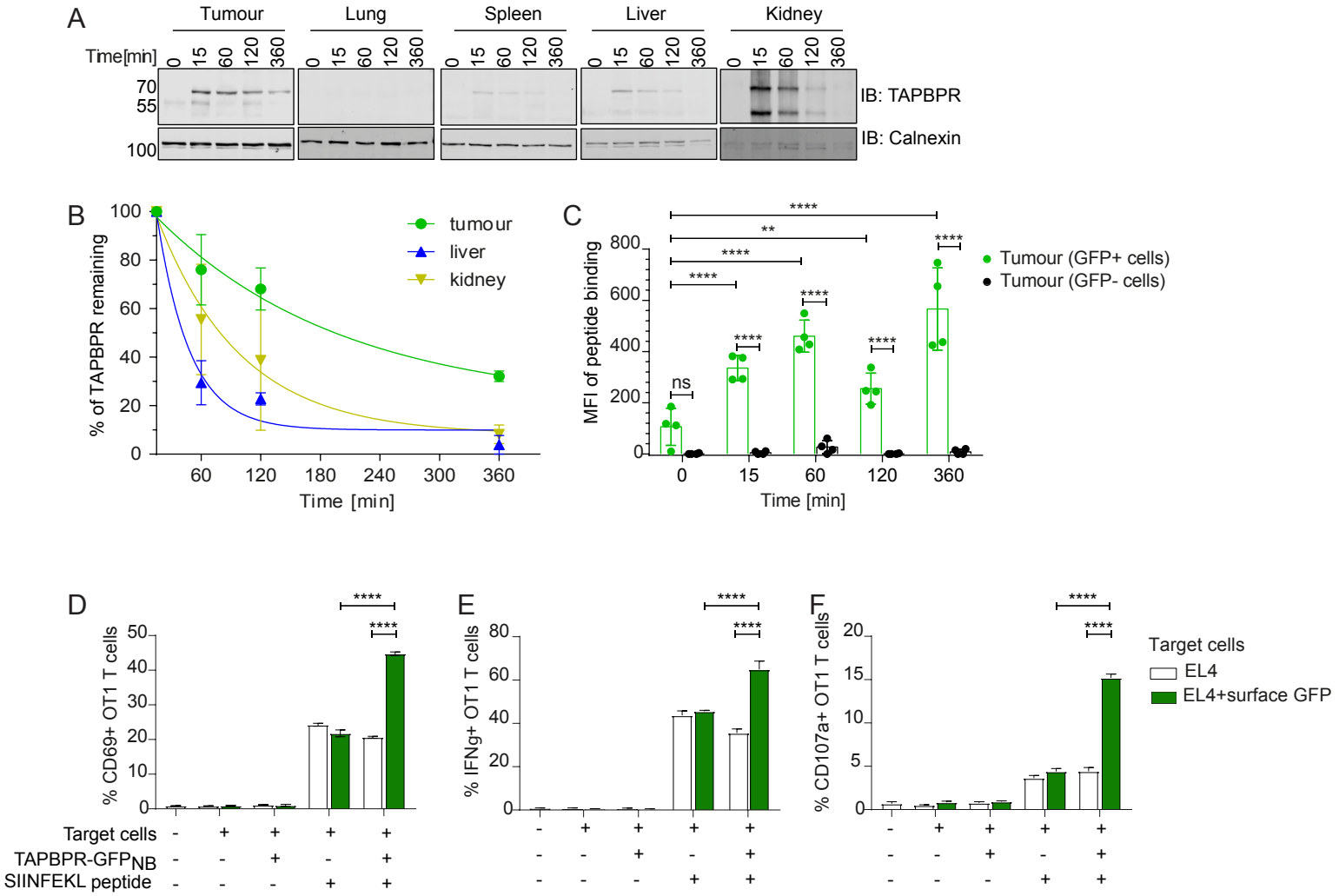
A
Tumour
Lung
Spleen
Liver
Kidney
Time[min]
0 15 60 120 360
70
55
100
IB: TAPBPR
IB: Calnexin
B
% of TAPBPR remaining
Time [min]
tumour
liver
kidney
C
MFI of peptide binding
Time [min]
ns
Tumour (GFP+ cells)
Tumour (GFP- cells)
D
% CD69+ OT1 T cells
E
% IFNg+ OT1 T cells
F
% CD107a+ OT1 T cells
Target cells
EL4
EL4+surface GFP
Target cells
TAPBPR-GFPNB
SIINFEKL peptide

Figure 4

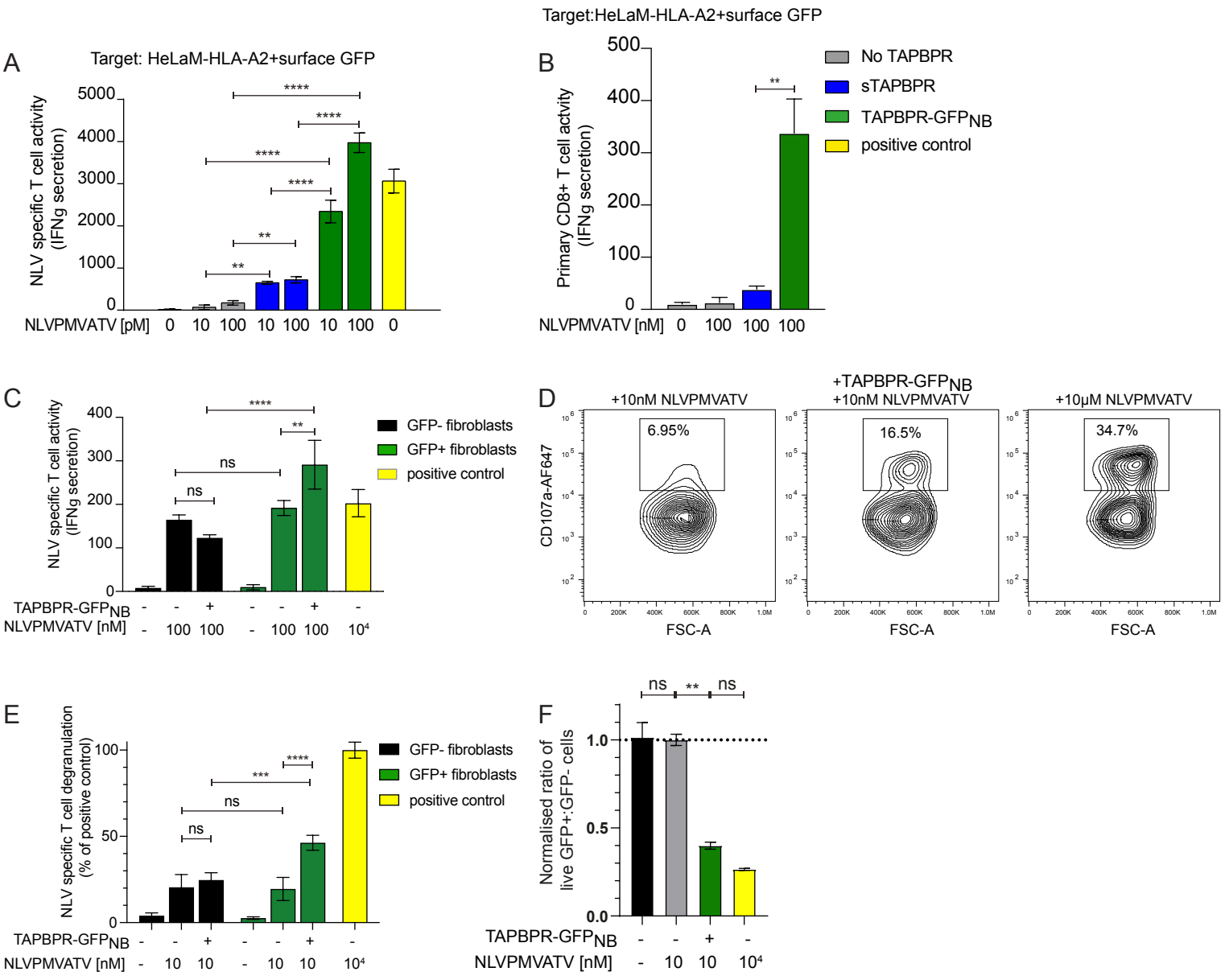
A
Target: HeLaM-HLA-A2+surface GFP
NLV specific T cell activity (IFNg secretion)
NLVPMVATV [pM] 0 10 100 10 100 10 100 0
B
Target:HeLaM-HLA-A2+surface GFP
Primary CD8+ T cell actvity (IFNg secretion)
No TAPBPR
sTAPBPR
TAPBPR-GFPNB
positive control
NLVPMVATV [nM] 0 100 100 100
C
NLV specific T cell activity (IFNg secretion)
GFP- fibroblasts
GFP+ fibroblasts
positive control
TAPBPR-GFPNB
NLVPMVATV [nM]
D
+TAPBPR-GFPNB
+10nM NLVPMVATV
+10nM NLVPMVATV
+10µM NLVPMVATV
CD107a-AF647
6.95%
16.5%
34.7%
FSC-A
E
NLV specific T cell degranulation (% of positive control)
GFP- fibroblasts
GFP+ fibroblasts
positive control
TAPBPR-GFPNB
NLVPMVATV [nM]
F
Normalised ratio of live GFP+:GFP- cells
TAPBPR-GFPNB
NLVPMVATV [nM]

Figure 5

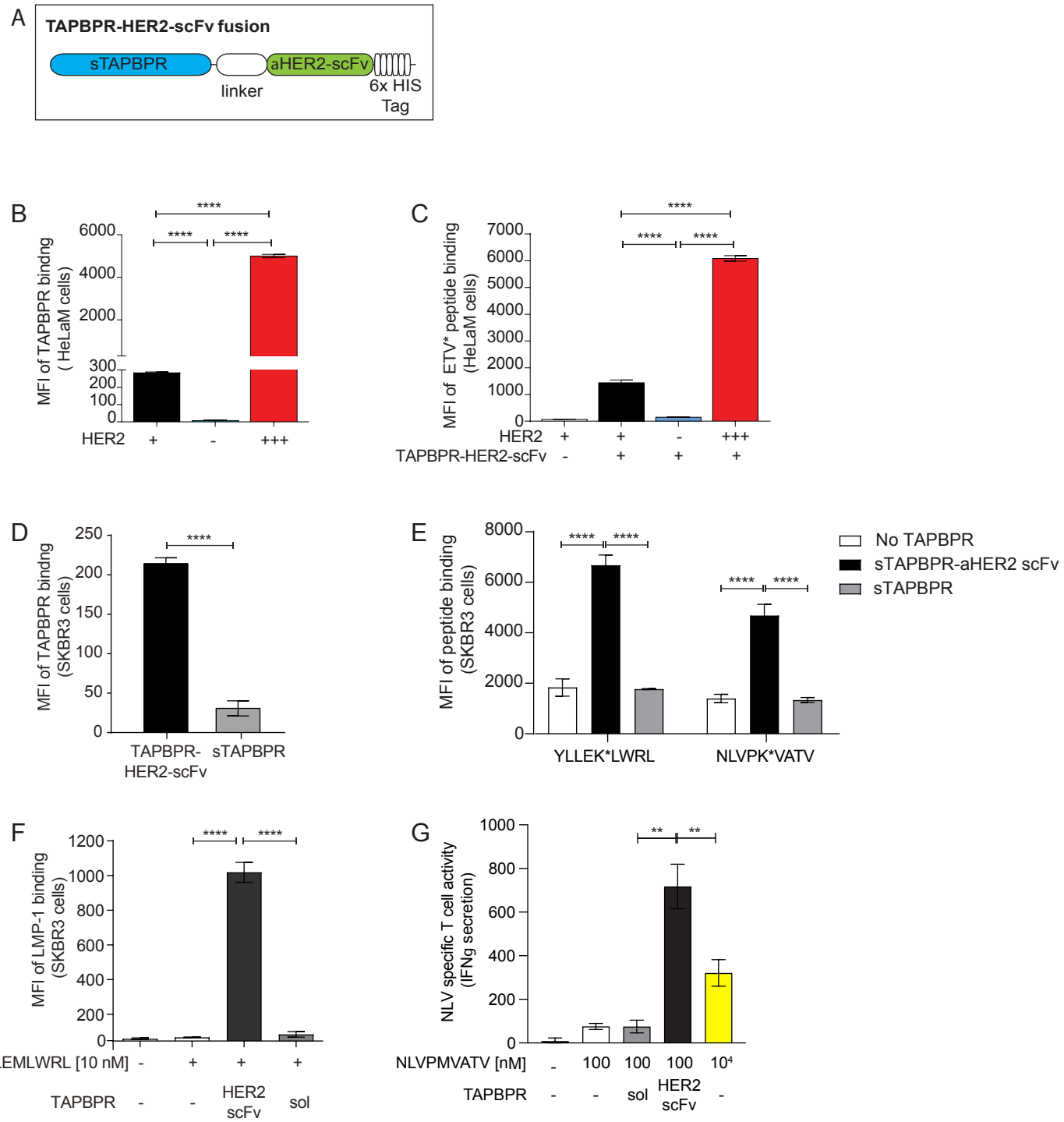
A
TAPBPR-HER2-scFv fusion
sTAPBPR
linker
aHER2-scFv
6x HIS Tag
B
MFI of TAPBPR binding ( HeLaM cells)
HER2 + - +++
C
MFI of ETV* peptide binding (HeLaM cells)
HER2 + + - +++
TAPBPR-HER2-scFv - + + +
D
MFI of TAPBPR binding (SKBR3 cells)
TAPBPR-HER2-scFv
sTAPBPR
E
MFI of peptide binding (SKBR3 cells)
YLLEK*LWRL
NLVPK*VATV
No TAPBPR
sTAPBPR-aHER2 scFv
sTAPBPR
F
MFI of LMP-1 binding (SKBR3 cells)
YLLEMLWRL [10 nM] - + + +
TAPBPR - - HER2 scFv sol
G
NLV specific T cell activity (IFNg secretion)
NLVPMVATV [nM] - 100 100 100 10⁴
TAPBPR - - sol HER2 scFv -

Figure 6

## Supplementary Files

This is a list of supplementary files associated with this preprint. Click to download.

- Combinedsupplementaryinfo8Dec22.pdf
- Combinedsupplementaryinfo8Dec22.pdf